

N-Heterocyclic carbene stabilized adducts of alkyl magnesium amide, bisalkyl magnesium and Grignard reagents: trapping oligomeric organo s-block fragments with NHCs†

Alan R. Kennedy, Robert E. Mulvey* and Stuart D. Robertson*

Received 21st June 2010, Accepted 4th August 2010

DOI: 10.1039/c0dt00693a

Developing N-heterocyclic carbene (NHC) chemistry of simple organomagnesium compounds, this study reports the synthesis, X-ray crystallographic, and NMR spectroscopic characterization of three such new carbene complexes. The 1 : 1 alkyl magnesium amide : carbene complexes $n\text{BuMg}(\text{TMP})\cdot\text{IPr}$ **1** and $n\text{BuMg}(\text{HMDS})\cdot\text{IPr}$ **2** both exist as mononuclear complexes in the crystal but differ in solution as **2** remains intact whereas **1** undergoes a dynamic exchange involving partial decoordination of IPr [TMP is 2,2,6,6-tetramethylpiperidide; IPr is 1,3-bis-(2,6-diisopropylphenyl)imidazol-2-ylidene]; HMDS is 1,1,1,3,3,3-hexamethyldisilazide]. Reaction of commercial $n\text{Bu}_2\text{Mg}$ with IPr surprisingly produced the organoaluminium carbene complex $n\text{Bu}_3\text{Al}\cdot\text{IPr}$, **3**, which also forms a simple mononuclear structure in the crystal. The presence of the Al could be traced to the deliberate addition of a small quantity of Et_3Al as a stabilizing agent in the commercial $n\text{Bu}_2\text{Mg}$ reagent. Repeating this reaction with Al-free $n\text{Bu}_2\text{Mg}$ afforded the hemisolvated carbene complex $n\text{Bu}_8\text{Mg}_4\cdot 2\text{IPr}$, **4**, the stoichiometry of which is dictated by its structure rather than by that used in the initial reaction mixture. The molecular structure of **4** is tetranuclear with a linear chain of 4 Mg centres bridged by $n\text{Bu}$ ligands and capped at each end by terminal $n\text{Bu}$ and IPr ligands. Synthesized by treating the Grignard reagent $n\text{BuMgCl}$ with IPr, $n\text{BuMgCl}\cdot\text{IPr}$, **5**, forms a cyclodimer structure with chloro bridges and terminal $n\text{Bu}$ and IPr ligands.

Introduction

Originally thought to be only transient intermediates which could not be isolated,¹ carbenes have advanced to the forefront of chemistry research in the past twenty years. Interest escalated after the groundbreaking discovery that they could be prepared as air-stable crystalline solids by incorporating the carbene centre into a heteroatomic ring and providing a large amount of steric protection.² These neutral N-heterocyclic carbene (NHC) species act as potent two electron σ -donors, one of their principal areas of utility being in catalysis³ where they can replace phosphines due to their greater nucleophilicity and consequently their stronger interactions with metal centres. One of their major attractions in catalysis is that carbenes can be subtly tuned by modifying the steric and electronic contributions of the N-bound organic groups. NHCs have consequently been studied in conjunction with virtually every metallic element of the periodic table.⁴ However, NHC chemistry of the s-block metals, particularly the alkaline earth metals, has seen much less attention than the transition metals. The group of Arnold,⁵ amongst others,⁶ has made progress in this territory by utilizing functionalized NHCs,⁷ which act as polydentate donors to magnesium *via* both neutral σ -donating divalent carbon centre(s) and also anionic arm(s) lying pendant

to the stabilizing heterocycle, while Alexakis has utilized such a functionalized NHC as a catalyst for asymmetric allylic alkylation with Grignard reagents although no structural intermediates were reported.⁸ Smith *et al.* have also exploited a tris(carbene)borate magnesium complex as a ligand transfer reagent.⁹ Pertinent to this study, only a handful of simpler monodentate neutral Mg-NHC complexes are known, which have generally been studied from the point of view of developing the chemistry of carbenes as opposed to using carbenes to advance alkaline earth metal chemistry. Arduengo¹⁰ prepared a pair of carbene adducts of the bis-alkyl Et_2Mg ; showing *via* single-crystal X-ray diffraction that one of these adducts exists as a dimer in the solid-state (**I**, Fig. 1); while a series of NHC stabilized dicyclopentadienyl group 2 metal complexes have also been synthesised (**II**).¹¹ A THF solvated structure of $\text{MgCl}_2\cdot\text{NHC}$ was also elucidated and recently reported (**III**),¹² while Roesky and Stalke recently divulged a bisalkynyl magnesium carbene adduct as a dimer (**IV**).¹³ Hill has prepared carbene adducts of $\text{M}[\text{N}(\text{SiMe}_3)_2]$ ($\text{M} = \text{Mg}, \text{Ca}, \text{Sr}, \text{Ba}$)¹⁴ as monomers (**V**) and subsequently has elegantly converted the Mg derivative to a Mg_4 hydride cluster (**VI**) which displays the highest H : Mg ratio of any such hydride to date and is dependent on the coordination of the NHC ligand for stability.^{14b}

Given the scarcity of Mg carbene adducts in the literature, particularly heteroleptic Mg species containing two distinct anions, coupled with our longstanding interest in s-block chemistry,¹⁵ we decided to pursue a series of such adducts with mixed alkyl-amido magnesium species. Thus we report herein the successful synthesis and solid-state structures of two new alkyl-amido magnesium carbene adducts. Further to this we shed some light on the potential structure of $n\text{Bu}_2\text{Mg}$, an important utility bis-alkyl magnesium reagent which has never before been characterized

WestCHEM, Department of Pure and Applied Chemistry, University of Strathclyde, Glasgow, UK, G1 1XL. E-mail: r.e.mulvey@strath.ac.uk; Fax: (+44) 141-5520876

† Electronic supplementary information (ESI) available: Synthetic protocol, molecular structure and CIF file for $[\text{BuMg}(\text{HMDS})]_2$ and CIF files for **1–5**. CCDC reference numbers 775962–775967. For ESI and crystallographic data in CIF or other electronic format see DOI: 10.1039/c0dt00693a

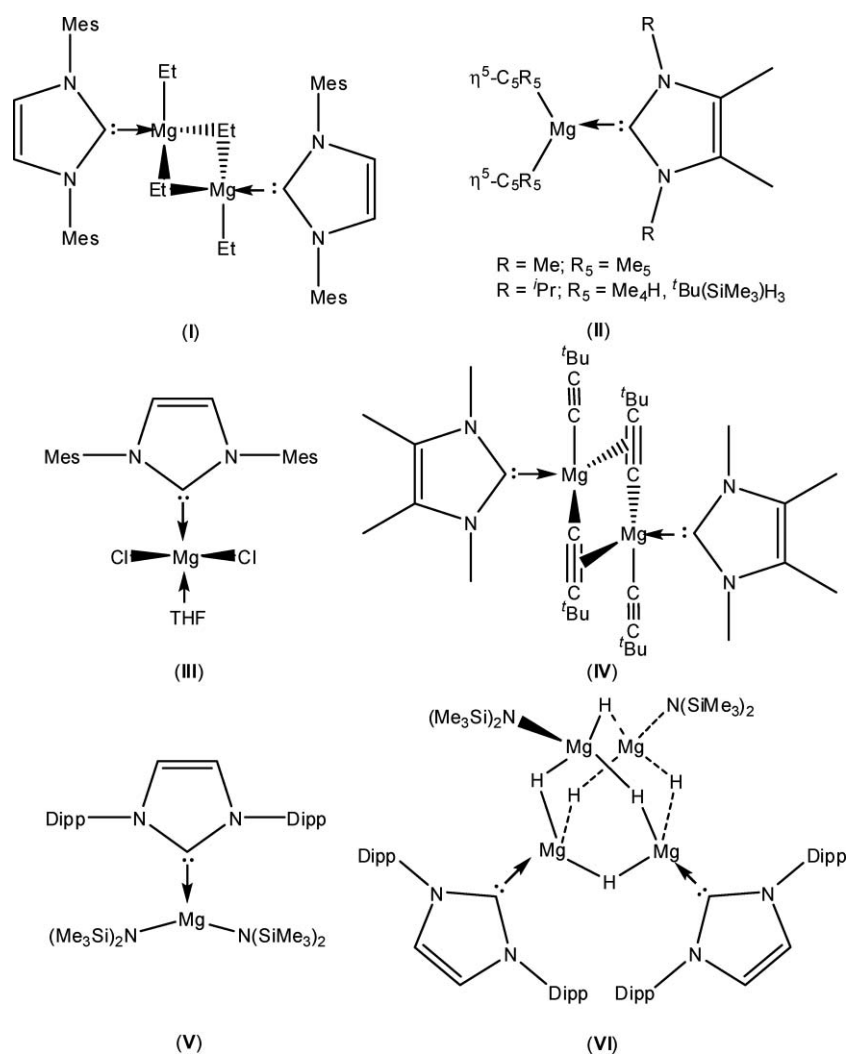


Fig. 1 Crystallography characterized carbene adducts of simple magnesium compounds.

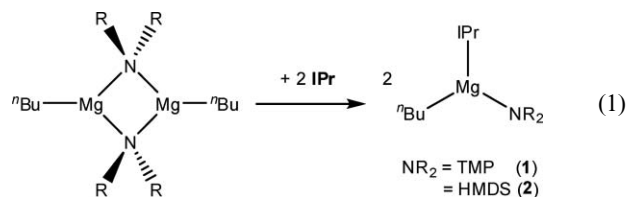
crystallographically either in the absence or presence of a donor, *via* identification of a novel carbene-stabilized modification whereby a linear $[\text{BuMg}]_4$ fragment has been trapped by two terminating carbene molecules. Finally, we also present the first crystallographically characterized carbene adduct of a Grignard (RMgCl) reagent as a dimer species containing a central planar Mg_2Cl_2 ring.

Results and discussion

Synthesis and solution studies of alkylamido magnesium carbene adducts 1 and 2

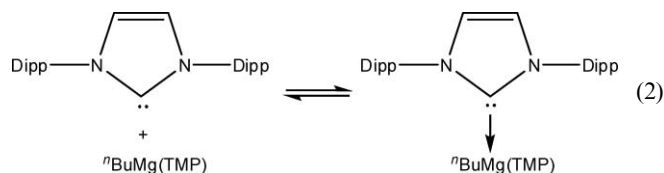
We commenced our study by pursuing a carbene stabilized alkyl magnesium amide adduct with the much studied utility base 2,2,6,6-tetramethylpiperidine (TMP) as the amide. Specifically, a sample of $\text{BuMg}(\text{TMP})$ was dissolved in a mixture of hexane and toluene and an equimolar amount of 1,3-bis-(2,6-diisopropylphenyl)imidazol-2-ylidene [IPr : chosen due to its ease of preparation and robustness of handling]¹⁶ was introduced. After stirring, the clear, pale yellow solution was cooled to -30°C . However, the crystals deposited were found by ^1H NMR spectroscopy

to be recrystallized IPr . This apparent failure of the carbene to coordinate to the electropositive metal was attributed to the combined steric bulk of the tBu and TMP ligands preventing the bulky carbene from gaining sufficient proximity. Consequently, we next examined the slightly less bulky $\text{tPrMg}(\text{TMP})$. Unfortunately, the crystalline product was again shown to be only IPr .



On moving to the linear $n\text{Bu}$ derivative of the alkyl Mg amide (eqn (1)), a crop of crystals developed whose ^1H and ^{13}C NMR spectra in C_6D_6 suggested that coordination of the carbene to the alkaline earth metal had occurred to give complex 1. Specifically, in the ^1H NMR spectrum, the olefinic unit and the tPr methine group resonated moderately upfield compared to those in the free carbene (6.49 and 2.82 ppm respectively; *cf.* 6.62 and 2.96 ppm in IPr)¹⁶ as did the Mg -bound CH_2 group of the $n\text{Bu}$ chain (-0.42 ppm,

cf. 0.05 in $[\text{t-BuMg}(\mu\text{-TMP})]_2$,¹⁷ while in the ^{13}C NMR spectrum the carbene carbon resonated at a frequency (189.7 ppm; *cf.* 220.6 ppm in IPr)¹⁶ typical for a coordinated carbene. This upfield shift of the Mg-CH₂ resonance has previously been attributed to the placement of these methylene protons in the shielding cone of the aromatic ring of the carbenes pendant arm, since the adamantyl substituted derivative of **1** did not cause such a shift.¹⁰ While the combination of TMP, ⁿBu and ⁱPr resonances made the aliphatic region of the ^1H spectrum complicated, all the hydrogen atoms in **1** could be assigned (see experimental section for complete details). However, of particular interest in these spectra were the presence of resonances attributable to both free IPr and also free $[\text{t-BuMg}(\text{TMP})]_2$, suggesting an equilibrium between the two starting materials and the adduct **1** was taking place (eqn (2)).



As mentioned earlier, the overlap caused by the multiple aliphatic resonances in the approximate range 0.95–2.00 ppm of the ^1H NMR spectrum meant that integration of these resonances was futile. However, the resonances representing the olefinic, *i*Pr CH and Mg-CH₂ fragments are sufficiently well separated for integration to be effective. Consequently, these regions were used to determine the relative amounts of each species in the equilibrium. The sample was subsequently subjected to a variable temperature ^1H NMR study (in C₇D₈), the results of which are displayed in Fig. S1 (ESI†). It initially appeared that as the temperature was reduced, the equilibrium shifted to the right, favouring the carbene adduct over the two starting materials while at 260 K this equilibrium reversed and began to favour the starting materials. However, when the variable temperature study was repeated with a sealed insert containing ferrocene as an integration standard, a depreciation in the relative amount of all three components of the equilibrium was witnessed, particularly of $[\text{t-BuMg}(\text{TMP})]_2$, suggesting that the results of this study are considerably altered by the precipitation of the alkyl magnesium amide species.

Next, we turned our attention to the carbene adduct of the related alkyl magnesium amide BuMg(HMDS). For consistency we utilized the ⁿBu derivative, which to the best of our knowledge has never been properly characterized. Its ^sBu isomer was reported by Raston *et al.* in 1986 as a dimer in the solid state.¹⁸ This product was formed in kinetic preference to the ⁿBu isomer when the parent amine HMDS(H) was reacted with an equimolar amount of the mixed alkyl magnesium reagent ^sBuMgⁿBu. Formed from a salt metathesis reaction of ^tBuMgCl and NaHMDS, the ^tBu isomer is also known to exist as a dimer.¹⁹ Our X-ray crystal study shows that the ⁿBu isomer, like the branched alkyl derivatives, is also a dimer in the solid state with terminal alkyl chains and bridging amido groups (see ESI Fig. S2 for full details†).

Stirring a solution of $[\text{t-BuMg}(\text{HMDS})]_2$ in the presence of IPr (eqn (1)) followed by cooling to –30 °C, resulted in crystals of **2**. Upon dissolution in C₆D₆, this product displayed NMR spectra consistent with a 1 : 1 adduct, with no evidence of either

starting material, suggesting that, unlike **1**, **2** is not undergoing a dynamic process in solution. As in the case of **1**, the most indicative resonances of a carbene adduct being formed were those of the olefin, methine and Mg-CH₂ functionalities (^1H NMR spectrum) and the carbene carbon (^{13}C NMR spectrum) which resonated at –0.33, 2.75, 6.40 and 187.0 ppm, respectively, all considerably shielded with respect to those of the starting materials $[\text{Mg-CH}_2$ of $[\text{t-BuMg}(\text{HMDS})]_2$ resonates at 0.05 ppm – ESI†] and are typical of carbene coordination.

Solid state structures of **1** and **2**

The molecular structures of the alkyl-amido magnesium carbene adducts **1** and **2** were elucidated *via* single-crystal X-ray diffraction and the results are displayed in Fig. 2 and 3, respectively while pertinent bond parameters are supplied in Table 1. Table 2 contains relevant crystallographic data.

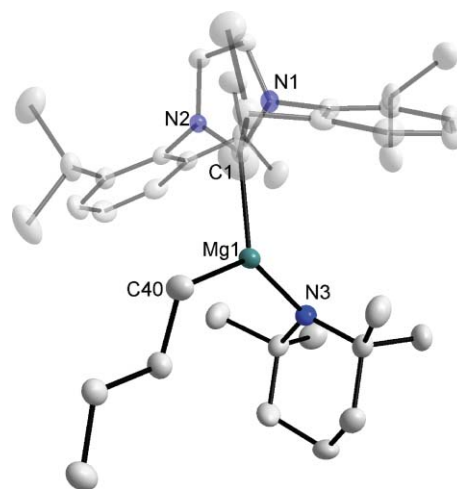


Fig. 2 Molecular structure of $[\text{t-BuMg}(\text{TMP})\cdot\text{IPr}]$ (**1**) with selected atom labels. Hydrogen atoms are omitted for clarity and thermal ellipsoids are displayed at the 50% probability level.

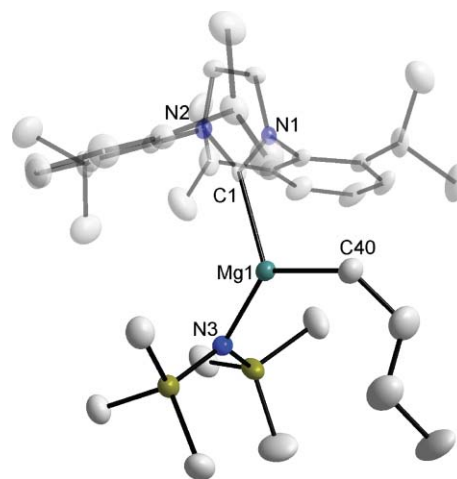


Fig. 3 Molecular structure of $[\text{t-BuMg}(\text{HMDS})\cdot\text{IPr}]$ (**2**) with selected atom labels. Hydrogen atoms are omitted for clarity and thermal ellipsoids are displayed at the 50% probability level.

Table 1 Selected bond lengths (Å) and angles (°) for **1** and **2**

	1	2		1	2
C(1)–N(1)	1.360(2)	1.363(3)	N(1)–C(1)–N(2)	103.1(1)	102.9(2)
C(1)–N(2)	1.362(2)	1.366(3)	N(1)–C(1)–Mg(1)	125.4(1)	127.3(2)
Mg(1)–C(1)	2.254(2)	2.268(2)	N(2)–C(1)–Mg(1)	130.0(1)	126.1(2)
Mg(1)–N(3)	1.980(1)	1.995(2)	C(1)–Mg(1)–N(3)	125.35(6)	125.6(1)
Mg(1)–C(40)	2.126(2)	2.140(2)	C(1)–Mg(1)–C(40)	108.77(7)	108.8(1)
			N(3)–Mg(1)–C(40)	125.87(4)	125.6(1)

Table 2 Crystallographic data and refinement details for compounds **1**, **2**, **3**, **4**, **5** and [BuMg(HMDS)]₂

	1 ^a	2	3	4	5	[BuMg(HMDS)] ₂
Empirical formula	C ₄₀ H ₆₃ MgN ₃	C ₃₇ H ₆₃ MgN ₃ Si ₂	C ₃₉ H ₆₃ AlN ₂	C ₃₆ H ₁₄₄ Mg ₄ N ₄	C ₆₂ H ₉₀ Cl ₂ Mg ₂ N ₄	C ₂₀ H ₅₄ Mg ₂ N ₂ Si ₄
Mol. Mass	610.24	630.39	586.89	1331.29	1010.90	483.63
Crystal system	Orthorhombic	Monoclinic	Triclinic	Monoclinic	Monoclinic	Monoclinic
Space group	<i>Pna</i> 2 ₁	<i>P</i> 2 ₁ / <i>c</i>	<i>P</i> 1	<i>P</i> 2 ₁ / <i>n</i>	<i>P</i> 2 ₁ / <i>n</i>	<i>C</i> 2/ <i>c</i>
<i>a</i> [Å]	18.7980(8)	18.5673(8)	9.5150(5)	17.5342(11)	12.5268(3)	16.3833(5)
<i>b</i> [Å]	11.7552(5)	11.0931(4)	10.4747(4)	13.7504(8)	14.3634(5)	11.1092(3)
<i>c</i> [Å]	17.4673(7)	19.6693(9)	19.0528(8)	17.7758(12)	35.1522(11)	17.1805(5)
α [°]	90	90	97.775(3)	90	90	90
β [°]	90	99.065(4)	97.597(4)	91.904(6)	97.089(2)	92.001(3)
γ [°]	90	90	93.331(4)	90	90	90
<i>V</i> [Å ³]	3859.8(3)	4000.7(3)	1859.37(14)	4283.4(5)	6276.5(3)	3125.04(16)
<i>Z</i>	4	4	2	2	4	4
λ [Å]	0.71073	0.71073	0.71073	1.5418	0.71073	0.71073
Measured reflections	16 084	41 501	16 290	21 729 ^b	36 444	11 966
Unique reflections	7556	9642	8474	21 729 ^b	12 334	4261
<i>R</i> _{int}	0.0333	0.0857	0.0519		0.0522	0.0264
Observed rflns [<i>I</i> > 2σ(<i>I</i>)]	5867	4962	4024	11 576	7550	3413
Goof	0.928	0.949	0.832	0.882	1.096	1.075
<i>R</i> [on <i>F</i> , obs rflns only]	0.0396	0.0652	0.0545	0.0638	0.0700	0.0466
<i>wR</i> [on <i>F</i> ² , all data]	0.0837	0.1255	0.0907	0.1760	0.2065	0.1224
Largest diff. peak/hole [e Å ⁻³]	0.259/−0.204	0.496/−0.290	0.253/−0.274	0.401/−0.294	0.649/−0.699	0.694/−0.268

^a Flack parameter refined to 0.35(12). ^b Total number of entries in HKLF 5 format dataset for a two component twin (rotation by 180° about 1 0 0).

As can be seen from these figures, the coordination of the carbene molecule to the Mg centre has broken up the dimeric alkyl magnesium amide species to generate a monomeric 1 : 1 adduct, consistent with the NMR data (*vide supra*). This results in a three-coordinate distorted trigonal planar metal centre ($\Sigma \angle \text{Mg} = 359.99^\circ$ **1**; 360.00° **2**). To alleviate steric strain, the amides and the carbene rings lie perpendicular to the plane defined by the trigonal planar MgL₃ unit. The plane of the carbene C₃N₂ ring lies at $89.10(7)^\circ$ and $86.99(9)^\circ$ to the C(1)–Mg(1)–C(40)–N(3) plane in **1** and **2**, respectively, while the plane generated by the NR₂ unit of the amide lies at $83.38(8)^\circ$ and $86.32(7)^\circ$ to the C(1)–Mg(1)–C(40)–N(3) plane in each case. The perpendicular relationships are facilitated by the lack of bulk associated with the linear alkyl ligand since these angles are considerably larger than the corresponding angles in the bulkier symmetric complex (HMDS)₂Mg·IPr (**V**) which are $50.64(5)^\circ$ and $79.06(4)^\circ$, respectively.^{14b}

The C_{carbene}–Mg distances in each case [**1**, 2.254(2) Å; **2**, 2.268(2) Å] are consistent with those witnessed in other such magnesium carbene adducts and are marginally shorter than in the bisamidomagnesium derivative **V** [2.276(2) Å], the closer proximity of the bulky carbene to the metal may again reflect the lower steric bulk of the linear ⁿBu ligand. The monomeric nature of the alkyl magnesium amide fragment in **1** and **2** results in a significant shortening of the Mg–N bond length [1.980(2) Å and 1.995(2) Å, respectively] since this nitrogen centre is no longer bridging two electropositive metals as is the case in the parent

alkylmagnesium amides [average Mg–N distances in the starting materials are 2.119 Å¹⁷ and 2.110 Å, respectively]. Unsurprisingly the terminal nature of the Mg–C bonds in both dimer and carbene adduct species means the Mg–C distances are almost identical. Complexes **1** and **2** represent rare examples of a three-coordinate Mg monomer of type Mg(L[−])₂·donor and are indeed the first such alkylamido derivatives.²⁰

Synthesis and solid state structure of bisalkyl magnesium carbene adduct **4**

Having successfully characterized a pair of alkyl-amido magnesium carbene adducts, we moved our attention to the carbene adduct of the related utility bis-alkyl magnesium species ⁿBu₂Mg. The synthesis of a similar 1 : 1 adduct appeared straight forward. Specifically, equimolar amounts of the two reagents were gently heated in hexane with stirring. The resulting crystalline product (**3**), which was formed in poor yield even after cooling to -70°C , was subjected to analysis both in solution and in the solid state. Its ¹H and ¹³C NMR spectra both displayed all the peaks expected for a coordinated IPr molecule (olefin and ¹Pr methine peaks at 6.41 and 2.74 ppm) and a ⁿBu group (M–CH₂: -0.35 ppm), however, the integration of these peaks suggested that three ⁿBu groups were present per molecule of IPr. To our surprise, rather than being a trimeric [ⁿBu₂Mg]₃ fragment with a capping carbene molecule at either end the solid state structure showed this to be a monomeric

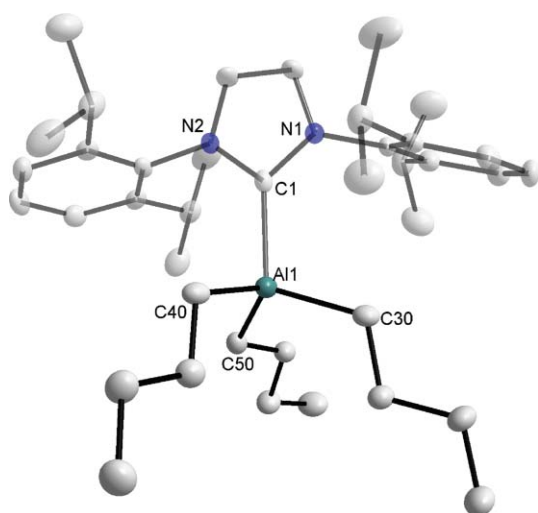


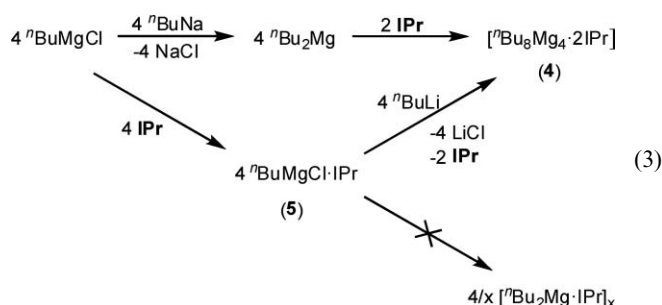
Fig. 4 Molecular structure of adventitious ${}^n\text{Bu}_3\text{Al}\cdot\text{IPr}$ (**3**) with selected atom labels. Hydrogen atoms are omitted for clarity and thermal ellipsoids are displayed at the 50% probability level. Selected bond lengths (Å) and angles ($^\circ$): C(1)–N(1) 1.364(2), C(1)–N(2) 1.373(2), Al(1)–C(1) 2.118(2), Al(1)–C(30) 1.993(2), Al(1)–C(40) 1.990(2), Al(1)–C(50) 1.996(2); N(1)–C(1)–N(2) 102.4(1), N(1)–C(1)–Al(1) 127.5(1), N(2)–C(1)–Al(1) 129.6(1), C(1)–Al(1)–C(30) 109.42(7), C(1)–Al(1)–C(40) 101.59(8), C(1)–Al(1)–C(50) 112.65(8), C(30)–Al(1)–C(40) 113.37(9), C(30)–Al(1)–C(50) 107.57(8), C(40)–Al(1)–C(50) 112.24(9).

adduct with three ${}^n\text{Bu}$ groups bound to the metal centre (Fig. 4). We initially postulated that this species was in fact a contacted ion pair imidazolium salt of formula $[\text{IPr}(\text{H})]^+ [{}^n\text{Bu}_3\text{Mg}]^-$. However, we could not find a satisfactory location for the extra proton on the carbene. The two most likely locations would be on the ‘carbene’ carbon or on the olefinic backbone; however, the solid state structure clearly shows that the ‘carbene’ carbon is trigonal planar (sp^2) and the NMR spectra suggested the carbene moiety is symmetric which would not be the case if the olefinic fragment was carrying an extra proton. The most reasonable explanation for this was that we had not actually formed a magnesium compound at all, but an aluminium ${}^n\text{Bu}_3\text{Al}$ carbene adduct. Such a hypothesis was supported by the metal–carbene bond, which was noticeably shorter [2.118(2) Å] than any previously determined Mg–carbene interaction. We subsequently confirmed this was the case by preparing an authentic sample of ${}^n\text{Bu}_3\text{Al}\cdot\text{IPr}$ from the analogous reaction of the tris-alkyl aluminium reagent with the parent carbene. A comparison of NMR spectra and unit cell parameters from X-ray crystallographic data confirmed that **3** was indeed ${}^n\text{Bu}_3\text{Al}\cdot\text{IPr}$. On inspection of the commercially purchased “ ${}^n\text{Bu}_2\text{Mg}$ ”, we found that it contains ~5–10% Et_3Al as a stabilising agent. It would therefore appear that alkyl exchange has occurred between the Al and Mg species, with the Al species being ‘trapped’ by the carbene, presumably due to the larger charge-density on the formally Al^{3+} trication. The Al species is then simply obtained by preferential crystallization. The poor yield mentioned earlier is attributable to the small amount of tris-alkyl aluminium present with respect to the bis-alkyl magnesium in solution.

The solid state structure of **3** represents a rare example of an aluminium carbene adduct (the majority of which are tri-hydride²¹ or tri-halide^{12,22} derivatives) and shows a distorted tetrahedral AlC_4 centre with the $\text{C}_{\text{carbene}}\text{--Al--C}_{\text{alkyl}}$ angles lying in the range 101.59(8)–

112.65(8) $^\circ$ and the $\text{C}_{\text{alkyl}}\text{--Al--C}_{\text{alkyl}}$ angles in the slightly narrower range 107.57(8)–113.37(9) $^\circ$. The $\text{C}_{\text{carbene}}\text{--Al}$ distance [2.118(2) Å] is noticeably longer than the $\text{C}_{\text{alkyl}}\text{--Al}$ distances [average 1.993 Å]. The $\text{C}_{\text{carbene}}\text{--Al}$ distance is consistent with that of the only other crystallographically characterized trialkyl aluminium adduct, that of $\text{Me}_3\text{Al}\cdot\text{carbene}$ (carbene = 1,3-diisopropyl-4,5-dimethylimidazol-2-ylidene) reported by Robinson *et al.* in 1996 [2.124(6) Å].²³ However, while the average $\text{C}_{\text{alkyl}}\text{--Al}$ bond length of **3** is similar to that in Robinson’s structure [2.001 Å], the methyl derivative shows a much wider range in such bond lengths [1.940(5)–2.062(7) Å]. In both cases, these bonds are longer than those of the only other carbene stabilized AlC_3 monomer, namely the trisalkynyl (${}^t\text{BuCC}$)₃Al·carbene (carbene = 1,3,4,5-tetramethylimidazol-2-ylidene) [average = 1.941 Å].²⁴

As a consequence of this unexpected complication, we decided to prepare our own ${}^n\text{Bu}_2\text{Mg}$ *in situ* and react it with IPr. For this preparation, a solution of ${}^n\text{BuMgCl}$ was slowly added to a stirring suspension of ${}^n\text{BuNa}$ in hexane at 0 $^\circ\text{C}$. After stirring overnight, this solution was filtered through Celite to remove precipitated NaCl and then an equimolar amount of IPr was introduced. The crude product obtained gave a ${}^1\text{H}$ NMR spectrum which displayed both coordinated and uncoordinated IPr in a 1 : 1 ratio. Broad resonances were witnessed for hydrogen atoms of the ${}^n\text{Bu}$ groups, with two resonances in the negative region of the spectrum at –0.1 and –0.6 ppm, with a relative integration of 1 : 3, suggesting that two different Mg– CH_2 environments (and thus at least two distinct ${}^n\text{Bu}$ groups) are present. Interestingly, complete integration suggested a total of four ${}^n\text{Bu}$ groups per carbene molecule. Matching this stoichiometry, this reaction was therefore repeated but with only half as much IPr added (eqn (3)). The recrystallised product (**4**) gave a ${}^1\text{H}$ NMR spectrum consistent with that previously seen, with the olefin and methine functionalities of the coordinated IPr molecule resonating at 6.37 and 2.81 ppm respectively. The molecular structure of **4** (Fig. 5) was elucidated by X-ray crystallography which showed it to be a centrosymmetric linear tetranuclear arrangement of ${}^n\text{Bu}_2\text{Mg}$ molecules with bridging ${}^n\text{Bu}$ groups, capped at either end with a combination of IPr and terminal ${}^n\text{Bu}$ groups.



This unexpected structure provides a rationale for the broad ${}^n\text{Bu}$ resonances in the ${}^1\text{H}$ NMR spectrum since three chemically and magnetically inequivalent ${}^n\text{Bu}$ groups are present as shown in Fig. 6. As mentioned earlier, the Mg– CH_2 resonances appear at –0.1 and –0.6 ppm in a 1 : 3 ratio. While it would be tempting to assign the major Mg– CH_2 resonance (–0.6 ppm) to the bridging butyl groups (that is $\text{Bu}^b + \text{Bu}^c$) and the minor resonance (–0.1 ppm) to the terminal butyl group (Bu^a), we surmise that the major resonance belongs to Bu^a and Bu^b (*i.e.* those which lie only two bonds from the carbene) while the minor resonance

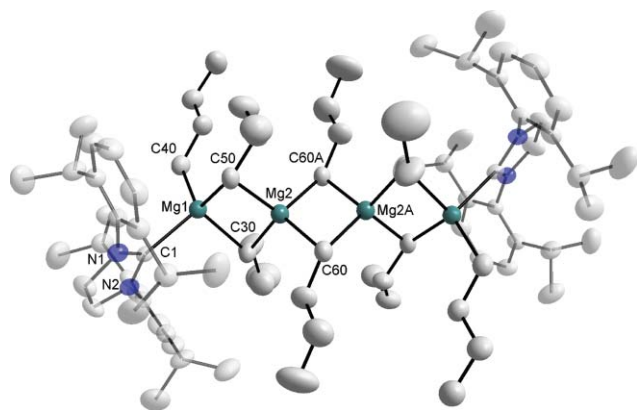


Fig. 5 Molecular structure of $[\text{Bu}_2\text{Mg}]_4 \cdot 2\text{IPr}$ (**4**) with selected atom labels. Hydrogen atoms are omitted for clarity and thermal ellipsoids are displayed at the 50% probability level. Symmetry transformations used to generate equivalent atoms: $2 - x$, $2 - y$, $-z$. Selected bond lengths (Å) and angles (°): C(1)–N(1) 1.372(3), C(1)–N(2) 1.367(3), Mg(1)–C(1) 2.285(2), Mg(1)–C(30) 2.303(3), Mg(1)–C(40) 2.143(3), Mg(1)–C(50) 2.342(2), Mg(2)–C(30) 2.229(3), Mg(2)–C(50) 2.207(3), Mg(2)–C(60) 2.250(3), Mg(2)–C(60A) 2.290(3); N(1)–C(1)–N(2) 103.1(2), N(1)–C(1)–Mg(1) 128.5(2), N(2)–C(1)–Mg(1) 128.3(2), C(1)–Mg(1)–C(30) 103.1(1), C(1)–Mg(1)–C(40) 117.0(1), C(1)–Mg(1)–C(50) 107.0(1), C(30)–Mg(1)–C(40) 115.3(1), C(30)–Mg(1)–C(50) 107.0(1), C(40)–Mg(1)–C(50) 111.6(1), Mg(1)–C(30)–Mg(2) 74.3(1), Mg(1)–C(50)–Mg(2) 73.9(1), C(30)–Mg(2)–C(50) 108.1(1), C(30)–Mg(2)–C(60) 113.7(1), C(30)–Mg(2)–C(60A) 103.7(1), C(50)–Mg(2)–C(60) 108.7(1), C(50)–Mg(2)–C(60A) 116.9(1), C(60)–Mg(2)–C(60A) 105.9(1), Mg(2)–C(60)–Mg(2A) 74.1(1).

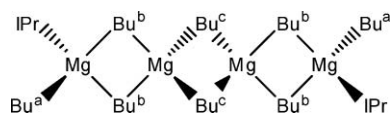


Fig. 6 Structure of **4** showing its distinct types of Bu ligand.

represents Bu^c which lies four bonds away from the carbene since an upfield shift is typical for a Mg-alkyl group upon coordination of a donor such as a carbene to the adjacent metal centre (*vide supra*).

This structure represents the first crystallographically characterized example of this important utility bis-alkyl magnesium species, the closest structure obtained thus far being TMEDA solvated $^n\text{Bu}_2\text{Mg}$, which crystallized preferentially from a solution of $^n\text{Bu}_2\text{Mg}$ containing both ^nBu and ^iBu ligands.²⁵ Other similar examples include a dioxane bridged polymer of $^{n\text{e}o}\text{Pe}_2\text{Mg}$,²⁶ a pair of $^n\text{Bu}_2\text{Mg}$ structures co-complexed with $\text{MO}^n\text{Bu}/\text{TMEDA}$ ($\text{M} = \text{Na}, \text{K}$)²⁷ and dianionic $[\text{Mg}^n\text{Bu}_4]^{2-}$ with DABCO bridged sodium cations [DABCO = diazabicyclo(2,2,2)octane].²⁸ The tetranuclear spirocyclic structure (**4**) shows two distinct Mg environments, both of which are distorted tetrahedral. The first [Mg(1)] has two bridging and one terminal ^nBu group with one carbene carbon completing the coordination sphere [range 103.1(1)–117.0(1)°] while the second [Mg(2)] simply has four bridging ^nBu groups attached [range 103.7(1)–116.9(1)°]. The central Mg_2C_2 ring is planar ($\Sigma = 360.0^\circ$) while the outer rings are slightly distorted from planarity ($\Sigma = 363.4^\circ$), probably as a consequence of the coordination of the bulky carbene to one of the Mg centres. The carbene–magnesium bond distance [2.285(2) Å] is consistent with

those of other¹⁰ alkyl magnesium carbene adducts (*vide supra*). Of the Mg-alkyl bond distances, the Mg(1)–C(40) bond (*i.e.* the terminal alkyl group) is unsurprisingly the shortest [2.143(3) Å]. Of the bridging alkyl–Mg bonds, there is a slight disparity in the bond distances. The longest are those attached to the carbene-bound magnesium centre [Mg(1)–C(30) 2.303(3) Å; Mg(1)–C(50) 2.342(2) Å], the elongation being a consequence of both electronic (electron donation from the carbene results in a marginally less electropositive Mg centre) and steric (the bulk of the carbene) reasons. The cumulative effect of this is seen in the Mg(2)–C(30) [2.229(3) Å] and Mg(2)–C(50) [2.207(3) Å] bonds, which are noticeably shorter. Finally, the internal Mg(2)–C(60) [2.250(3) Å] and Mg(2)–C(60A) [2.290(3) Å] bonds are intermediate between these two extremes and are closer to a typical Mg– $\text{C}_{\text{bridging}}$ bond length such as those witnessed in dimeric $[\text{Bu}_2\text{Mg}]_2$,²⁹ whose Mg– $\text{C}_{\text{bridging}}$ bond lengths display an average of 2.3016 Å.

Having ‘trapped’ a tetranuclear fragment of presumably polymeric $^n\text{Bu}_2\text{Mg}$, the ratio of starting materials was altered to 1 : 4 in an attempt to obtain a longer bis-alkyl magnesium chain. However, the resulting product was shown by ^1H NMR spectroscopy and comparison of its unit cell parameters to indeed be **4**, suggesting that this tetranuclear structure is produced regardless of the ratio of the starting materials.

Since there appears to be no steric reason why a 1 : 1 carbene adduct of $^n\text{Bu}_2\text{Mg}$ cannot exist; either as a monomer such as **1** or **2**, or a dimer such as the ethyl derivative **I**; we propose that the oligomeric form of **4** occurs predominantly as a consequence of electronic factors. An attempt was therefore made to prepare a 1 : 1 adduct *via* an alternative pathway, namely by preparing a 1 : 1 carbene adduct of the related Grignard reagent $^n\text{BuMgCl}$ (**5**) and then replacing the chloride anion with another ^nBu group *via* a simple salt metathesis using $^n\text{BuLi}$ according to eqn (3).

The intermediate Grignard adduct **5** was isolated as large crystals upon slowly cooling to room temperature of a warmed hexane solution containing an equimolar amount of $^n\text{BuMgCl}$ and IPr. As in the case of the previously discussed Mg carbene adducts, the principal resonances of interest in the ^1H NMR spectrum were those of the olefin (6.42 ppm) and methine (2.83 ppm) functionalities of the carbene and the metal bound CH_2 fragment (−0.62 ppm), while the carbene carbon resonated at 188.1 ppm in the ^{13}C spectrum. There was no evidence of uncoordinated IPr. Integration of the butyl resonances with respect to those of the carbene indicated that one ^nBu group was present per carbene. One of the resonances representing another CH_2 of the ^nBu group could not be resolved in the ^1H spectrum, however a HSQC experiment confirmed that it was present and was in fact hidden under one of the doublets representing a methyl group of the carbene ^iPr arm.

The 1 : 1 nature of this product was confirmed *via* its molecular structure (Fig. 7) which showed that in this case the Grignard reagent dimerizes with its chloride anions in the bridging position, resulting in a pair of four-coordinate distorted tetrahedral magnesium centres and a central four-membered Mg_2Cl_2 ring. Due to disorder in the organic periphery of this non-centrosymmetric structure a detailed description of its bond parameters is unwarranted. The structure does however show that the Mg_2Cl_2 ring is planar, with the Mg centres displaying distorted tetrahedral geometry. The C_3N_2 ring of the heterocyclic carbene lies approximately coplanar with the plane of the two chlorine anions, resulting in

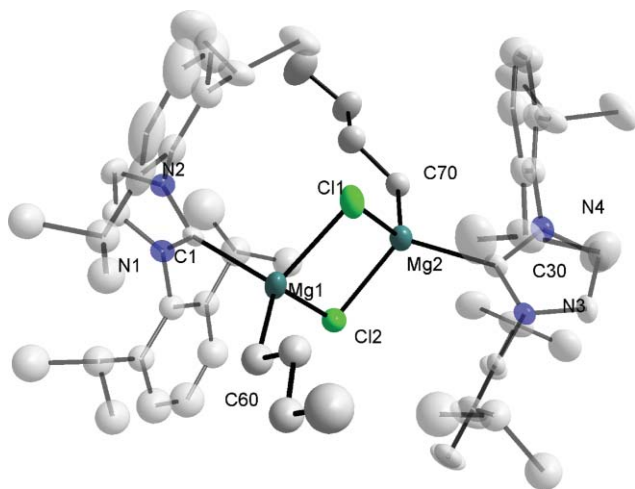


Fig. 7 Molecular structure of $[\text{n-BuMgCl} \cdot \text{IPr}]_2$ (**5**) with selected atom labels. Hydrogen atoms are omitted for clarity and thermal ellipsoids are displayed at the 50% probability level. This structure is disordered over one of the n-Bu groups and the carbene ligands, but only one component is shown.

the bulky 2,6-diisopropylphenyl groups protecting these otherwise exposed anions by provide steric shielding above and below them.

The metathetical reaction of **5** with n-BuLi (eqn (3)) was then carried out in hexane at room temperature. A white precipitate, presumably LiCl , was noticed as soon as the alkyl lithium reagent was added. This was filtered and the resulting solution was cooled to -30°C to precipitate crystals which were shown by NMR spectroscopy and X-ray diffraction to be the previously discussed **4** suggesting that the metathesis reaction to form putative monomeric “ $\text{n-Bu}_2\text{Mg} \cdot \text{IPr}$ ” has taken place with oligomerization and loss of some IPr ligand to generate the tetranuclear magnesium chain species **4**.

Conclusion

This study has considerably expanded upon the limited previous reports of magnesium carbene adducts, principally through the preparation of a pair of monomeric alkylmagnesium amide complexes with a carbene donor. We have also, to the best of our knowledge, established a new application for N-heterocyclic carbenes, namely as trapping agents for oligomeric fragments of organometallic polymers³⁰ that, by extrapolation, could provide valuable insight into the numerous unknown structures of solvent-free organo-s-block (especially important lithium and magnesium) compounds, many of which are suspected of being polymeric but which remain to be structurally elucidated. Further to this we have characterized for the first time a carbene stabilized Grignard reagent and also revealed a potential problem in organomagnesium chemistry; that is the potential of aluminium containing compounds, used as stabilizing agents in commercial organomagnesium samples, to preferentially react and give unusual or unexpected results which cannot be conventionally explained.

Experimental section

General

All reactions and manipulations were carried out under a protective argon atmosphere using either standard Schlenk techniques or a glove box. All solvents were dried over Na/benzophenone and freshly distilled prior to use. IPr^{16} and $[\text{n-BuMg}(\text{TMP})]_2^{17}$ were prepared according to literature methods. $\text{n-Bu}_2\text{Mg}$ and n-BuMgCl were purchased from Aldrich and used as received while $\text{n-Bu}_3\text{Al}$ was purchased from Alfa-Aesar and used as received. ^1H and ^{13}C NMR spectra were recorded on a Bruker AV400 MHz spectrometer (operating at 400.03 MHz for ^1H and 100.58 MHz for ^{13}C). All ^{13}C NMR spectra were proton decoupled. Satisfactory elemental analyses could not be obtained due to the sensitive nature of the compounds, evidence of purity is provided *via* ^1H NMR spectra (see Fig. S3–S7 in the ESI† and below for full assignments).

Synthesis of $\text{n-BuMg}(\text{TMP}) \cdot \text{IPr}$ (**1**)

Hexane (5 mL) was added *via* syringe to a mixture of $\text{n-BuMg}(\text{TMP})$ (0.111 g, 0.5 mmol) and IPr (0.194 g, 0.5 mmol). Toluene was then added dropwise, with sonication, until a homogeneous solution was obtained. This was cooled to -30°C where colourless crystals (0.171 g, 56%) developed. ^1H NMR (400.13 MHz, C_6D_6 , 300 K): -0.42 (t, 2H, $^2J_{\text{H,H}} = 8$ Hz, Mg-CH_2), 0.97 (s, 12H, TMP Me), 0.98 (d, 12H, $^2J_{\text{H,H}} = 7$ Hz, CHMe_2), 1.21 (t, 9H, $^2J_{\text{H,H}} = 7$ Hz, $\text{CH}_2\text{CH}_2\text{CH}_3$), 1.44 (d, 12H, $^2J_{\text{H,H}} = 7$ Hz, CHMe_2) [β CH_2 (TMP) hidden under this (shown by HSQC) – integral actually adds up to 16 (12 + 4)], 1.73 (sex, 2H, $^2J_{\text{H,H}} = 7$ Hz, $\text{CH}_2\text{CH}_2\text{CH}_3$), 1.89 (m, 4H, $\text{CH}_2\text{CH}_2\text{CH}_3$ and TMP γ CH_2), 2.82 (sept, 4H, $^2J_{\text{H,H}} = 7$ Hz, CHMe_2), 6.49 (s, 2H, olefin), 7.11 (d, 4H, $^2J_{\text{H,H}} = 8$ Hz, *meta* CH), 7.21 (t, 2H, $^2J_{\text{H,H}} = 8$ Hz, *para* CH). $^{13}\text{C}\{^1\text{H}\}$ NMR (100.58 MHz, C_6D_6 , 300 K): 11.8 (Mg-CH_2), 14.5 ($\text{CH}_2\text{CH}_2\text{CH}_3$), 20.8 (γ CH_2 TMP), 23.4 (CHMe_2), 25.8 (CHMe_2), 28.8 (CHMe_2), 32.3 ($\text{CH}_2\text{CH}_2\text{CH}_3$), 33.6 ($\text{CH}_2\text{CH}_2\text{CH}_3$), 34.2 (TMP Me), 40.7 (β CH_2 TMP), 51.6 (α C TMP), 123.7 (olefin), 124.4 (*meta* CH), 130.7 (*para* CH), 135.7 (*ipso*), 146.1 (*ortho*), 189.7 (carbene).

Synthesis of $\text{n-BuMg}(\text{HMDS}) \cdot \text{IPr}$ (**2**)

This complex was prepared using the same method as described above for **1** using $\text{n-BuMg}(\text{HMDS})$ (0.121 g, 0.5 mmol) in place of $\text{n-BuMg}(\text{TMP})$. This was cooled to -70°C to give a crop of colourless crystals (0.236 g, 75%). ^1H NMR (400.13 MHz, C_6D_6 , 300 K): -0.33 (t, 2H, $^2J_{\text{H,H}} = 8$ Hz, Mg-CH_2), 0.01 (s, 18H, SiMe_3), 0.97 (d, 12H, $^2J_{\text{H,H}} = 7$ Hz, CHMe_2), 1.20 (t, 3H, $^2J_{\text{H,H}} = 7$ Hz, $\text{CH}_2\text{CH}_2\text{CH}_3$), 1.41 (d, 12H, $^2J_{\text{H,H}} = 7$ Hz, CHMe_2), 1.70 (sex, 2H, $^2J_{\text{H,H}} = 7$ Hz, $\text{CH}_2\text{CH}_2\text{CH}_3$), 1.89 (quin, 2H, $^2J_{\text{H,H}} = 8$ Hz, $\text{CH}_2\text{CH}_2\text{CH}_3$), 2.75 (sept, 4H, $^2J_{\text{H,H}} = 7$ Hz, CHMe_2), 6.40 (s, 2H, olefin), 7.10 (d, 4H, $^2J_{\text{H,H}} = 8$ Hz, *meta* CH), 7.21 (t, 2H, $^2J_{\text{H,H}} = 8$ Hz, *para* CH). $^{13}\text{C}\{^1\text{H}\}$ NMR (100.58 MHz, C_6D_6 , 300 K): 4.8 (SiMe_3), 10.7 (Mg-CH_2), 14.3 ($\text{CH}_2\text{CH}_2\text{CH}_3$), 23.4 (CHMe_2), 25.3 (CHMe_2), 28.6 (CHMe_2), 31.8 ($\text{CH}_2\text{CH}_2\text{CH}_3$), 32.8 ($\text{CH}_2\text{CH}_2\text{CH}_3$), 124.0 (olefin), 124.5 (*meta* CH), 130.8 (*para* CH), 135.3 (*ipso*), 145.8 (*ortho*), 187.0 (carbene).

Synthesis of ⁿBu₃Al·IPr (3)

ⁿBu₃Al (0.5 mL, 0.7M in heptane, 0.35 mmol) was added *via* syringe to a suspension of IPr (0.136 g, 0.35 mmol) to yield a white suspension. Toluene was added dropwise with stirring until homogeneous. Upon cooling to −30 °C a crop of colourless crystals developed (0.144 g, 70%). ¹H NMR (400.13 MHz, C₆D₆, 300 K): −0.35 (t, 6H, ²J_{H,H} = 8 Hz, Al–CH₂), 0.96 (d, 12H, ²J_{H,H} = 7 Hz, CHMe₂), 1.03 (t, 9H, ²J_{H,H} = 7 Hz CH₂CH₂CH₃), 1.43 (d, 12H, ²J_{H,H} = 7 Hz, CHMe₂), 1.49 (m, 12H, CH₂CH₂CH₃) 2.74 (sept, 4H, ²J_{H,H} = 7 Hz, CHMe₂), 6.41 (s, 2H, olefin), 7.13 (d, 4H, ²J_{H,H} = 8 Hz, *meta* CH), 7.26 (t, 2H, ²J_{H,H} = 8 Hz, *para* CH). ¹³C{¹H} NMR (100.58 MHz, C₆D₆, 300 K): 10.5 (Al–CH₂), 14.4 (CH₂CH₂CH₃), 22.7 (CHMe₂), 26.0 (CHMe₂), 28.9 (CHMe₂), 30.4 (CH₂CH₂CH₃), 124.1 (*meta* CH), 124.5 (olefin), 130.7 (*para* CH), 135.7 (*ipso*), 145.9 (*ortho*), 191.0 (carbene).

Synthesis of ⁿBu₈Mg₄·2IPr (4)

ⁿBuMgCl (0.5 mL, 2M in Et₂O, 1 mmol) was added *via* syringe to a suspension of ⁿBuNa (0.080 g, 1 mmol) in hexane (5 mL) at 0 °C. After stirring overnight, this mixture was filtered through Celite to remove NaCl and washed with more hexane (2 × 5 mL). IPr (0.194 g, 0.5 mmol) was added from a solid addition tube and stirred. Toluene was added dropwise until a homogeneous solution was obtained and this was cooled to −30 °C to precipitate a crop of colourless crystals. (0.283 g, 85%). ¹H NMR (400.13 MHz, C₆D₆, 300 K): −0.6 (br, 24H, Mg–CH₂ × 6), −0.1 (br, 4H, Mg–CH₂ × 2), 0.98 (d, 12H, ²J_{H,H} = 7 Hz, CHMe₂), 1.1 (br, 24H, CH₂CH₂CH₃ × 8), 1.44 (d, 24H, ²J_{H,H} = 7 Hz, CHMe₂), 1.7 (br, 32H, CH₂CH₂CH₃ × 8), 2.81 (sept, 8H, ²J_{H,H} = 7 Hz, CHMe₂), 6.37 (s, 4H, olefin), 7.13 (d, 8H, ²J_{H,H} = 8 Hz, *meta* CH), 7.26 (t, 4H, ²J_{H,H} = 8 Hz, *para* CH). ¹³C{¹H} NMR (100.58 MHz, C₆D₆, 300 K): 10.2 (Mg–CH₂), 14.5 (CH₂CH₂CH₃), 23.5 (CHMe₂), 25.7 (CHMe₂), 28.8 (CHMe₂), 32.0 (CH₂CH₂CH₃), 124.1 (olefin), 124.4 (*meta* CH), 130.7 (*para* CH), 136.1 (*ipso*), 145.8 (*ortho*), 197.3 (carbene).

Synthesis of ⁿBuMgCl·IPr (5)

ⁿBuMgCl (0.25 mL, 2M in Et₂O, 0.5 mmol) was added *via* syringe to a suspension of IPr (0.194 g, 0.5 mmol) in hexane (5 mL). This initially gave a clear solution until a white precipitate formed after 2 min of stirring. The suspension was heated until homogeneous and slowly cooled to room temperature overnight in a Dewar flask of hot water to yield a crop of colourless crystals (0.187 g, 74%). ¹H NMR (400.13 MHz, C₆D₆, 300 K): −0.62 (t, 2H, ²J_{H,H} = 9 Hz, Mg–CH₂), 0.98 (d, 12H, ²J_{H,H} = 7 Hz, CHMe₂), 1.24 (t, 3H, ²J_{H,H} = 7 Hz CH₂CH₂CH₃), 1.46 (d, 12H, ²J_{H,H} = 7 Hz, CHMe₂), 1.46 (m, 2H, CH₂CH₂CH₃) 1.59 (sex, 2H, CH₂CH₂CH₃), 2.83 (sept, 4H, ²J_{H,H} = 7 Hz, CHMe₂), 6.42 (s, 2H, olefin), 7.13 (d, 4H, ²J_{H,H} = 7 Hz, *meta* CH), 7.26 (t, 2H, ²J_{H,H} = 7 Hz, *para* CH). ¹³C{¹H} NMR (100.58 MHz, C₆D₆, 300 K): 10.3 (Mg–CH₂), 14.8 (CH₂CH₂CH₃), 23.2 (CHMe₂), 25.8 (CHMe₂), 28.8 (CHMe₂), 32.7 (CH₂CH₂CH₃), 33.1 (CH₂CH₂CH₃), 123.9 (olefin), 124.1 (*meta* CH), 130.3 (*para* CH), 135.8 (*ipso*), 145.8 (*ortho*), 188.1 (carbene).

X-Ray diffraction data

Crystallographic data was collected at 123(2) K on Oxford Diffraction instruments. Structures were refined to convergence

against *F*² and all independent reflections by the full-matrix least-squares method using the *SHELXL-97* program.³¹ Selected crystallographic and refinement parameters are given in Table 2. CCDC 775962–775967 contain the supplementary crystallographic data for this paper.†

Acknowledgements

We would like to thank the UK EPSRC (through grant awards EP/F063733/1 and EP/D076889/1) and the Royal Society (through a Wolfson merit award to R.E.M.).

References

- For a excellent review of the pursuit of the first stable NHC see: F. E. Hahn and M. C. Jahnke, *Angew. Chem., Int. Ed.*, 2008, **47**, 3122–3172.
- A. J. Arduengo III, R. L. Harlow and M. Kline, *J. Am. Chem. Soc.*, 1991, **113**, 361–363.
- (a) S. Diez-González, N. Marion and S. P. Nolan, *Chem. Rev.*, 2009, **109**, 3612–3676; (b) X. Bantreil, J. Broggi and S. P. Nolan, *Annu. Rep. Prog. Chem., Sect. B: Org. Chem.*, 2009, **105**, 232–263.
- D. Bourissou, O. Guerret, F. P. Gabbaï and G. Bertrand, *Chem. Rev.*, 2000, **100**, 39–91.
- (a) S. A. Mungur, S. T. Liddle, C. Wilson, M. J. Sarsfield and P. L. Arnold, *Chem. Commun.*, 2004, 2738–2739; (b) P. L. Arnold, I. S. Edworthy, C. D. Carmichael, A. J. Blake and C. Wilson, *Dalton Trans.*, 2008, 3739–3746; (c) P. L. Arnold, I. J. Casely, Z. R. Turner, R. Bellabarba and R. B. Tooze, *Dalton Trans.*, 2009, 7236–7247.
- D. Zhang and H. Kawaguchi, *Organometallics*, 2006, **25**, 5506–5509.
- O. Kühn, *Chem. Soc. Rev.*, 2007, **36**, 592–607.
- O. Jackowski and A. Alexakis, *Angew. Chem., Int. Ed.*, 2010, **49**, 3346–3350.
- I. Nieto, F. Cervantes-Lee and J. M. Smith, *Chem. Commun.*, 2005, 3811–3813.
- A. J. Arduengo III, H. V. R. Dias, F. Davidson and R. L. Harlow, *J. Organomet. Chem.*, 1993, **462**, 13–18.
- (a) A. J. Arduengo III, F. Davidson, R. Krafczyk, W. J. Marshall and M. Tamm, *Organometallics*, 1998, **17**, 3375–3382; (b) H. Schumann, J. Gottfriedsen, M. Glanz, S. Dechert and J. Demtschuk, *J. Organomet. Chem.*, 2001, **617–618**, 588–600.
- B. Bantu, G. M. Pawar, K. Wurst, U. Decker, A. M. Schmidt and M. R. Buchmeiser, *Eur. J. Inorg. Chem.*, 2009, 1970–1976.
- A. Stasch, S. P. Sarish, H. W. Roesky, K. Meindl, F. Dall’Antonia, T. Schulz and D. Stalke, *Chem.–Asian J.*, 2009, **4**, 1451–1457.
- (a) A. G. M. Barrett, M. R. Crimmin, M. S. Hill, G. Kociok-Köhn, D. J. MacDougall, M. F. Mahon and P. A. Procopiou, *Organometallics*, 2008, **27**, 3939–3946; (b) M. Arrowsmith, M. S. Hill, D. J. MacDougall and M. F. Mahon, *Angew. Chem., Int. Ed.*, 2009, **48**, 4013–4016.
- (a) R. Forret, A. R. Kennedy, J. Klett, R. E. Mulvey and S. D. Robertson, *Organometallics*, 2010, **29**, 1436–1442; (b) W. Clegg, B. Conway, P. García-Álvarez, A. R. Kennedy, R. E. Mulvey, L. Russo, J. Saßmannshausen and T. Tuttle, *Chem.–Eur. J.*, 2009, **15**, 10702–10706; (c) J. García-Álvarez, D. V. Graham, E. Hevia, A. R. Kennedy and R. E. Mulvey, *Dalton Trans.*, 2008, 1481–1486.
- A. J. Arduengo III, R. Krafczyk, R. Schmutzler, H. A. Craig, J. R. Goerlich, W. J. Marshall and M. Unverzagt, *Tetrahedron*, 1999, **55**, 14523–14534.
- E. Hevia, A. R. Kennedy, R. E. Mulvey and S. Weatherstone, *Angew. Chem., Int. Ed.*, 2004, **43**, 1709–1712.
- L. M. Englehart, B. S. Jolly, P. C. Junk, C. L. Raston, B. W. Skelton and A. H. White, *Aust. J. Chem.*, 1986, **39**, 1337–1345.
- B. Conway, E. Hevia, A. R. Kennedy, R. E. Mulvey and S. Weatherstone, *Dalton Trans.*, 2005, 1532–1544.
- (a) A. R. Kennedy, R. E. Mulvey and J. H. Schulte, *Acta Crystallogr., Sect. C: Cryst. Struct. Commun.*, 2001, **57**, 1288–1289; (b) A. C. Avent, C. F. Caro, P. B. Hitchcock, M. F. Lappert, Z. Li and X.-H. Wei, *Dalton Trans.*, 2004, 1567–1577; (c) X. He, J. J. Morris, B. C. Noll, S. N. Brown and K. W. Henderson, *J. Am. Chem. Soc.*, 2006, **128**, 13599–13610.
- (a) A. J. Arduengo III, H. V. R. Dias, J. C. Calabrese and F. Davidson, *J. Am. Chem. Soc.*, 1992, **114**, 9724–9725; (b) R. J. Baker, A. J. Davies, C. Jones and M. Kloth, *J. Organomet. Chem.*, 2002, **656**, 203–210; (c) R.

- J. Baker, M. L. Cole, C. Jones and M. F. Mahon, *J. Chem. Soc., Dalton Trans.*, 2002, 1992–1996.
- 22 (a) A. Stasch, S. Singh, H. W. Roesky, M. Noltemeyer and H.-G. Schmidt, *Eur. J. Inorg. Chem.*, 2004, 4052–4055; (b) R. S. Ghadwal, H. W. Roesky, R. Herbst-Irmer and P. G. Jones, *Z. Anorg. Allg. Chem.*, 2009, **635**, 431–433.
- 23 X.-W. Li, J. Su and G. H. Robinson, *Chem. Commun.*, 1996, 2683–2684.
- 24 M. Schiefer, N. D. Reddy, H.-J. Ahn, A. Stasch, H. W. Roesky, A. C. Schlicker, H.-G. Schmidt, M. Noltemeyer and D. Vidovic, *Inorg. Chem.*, 2003, **42**, 4970–4976.
- 25 N. D. R. Barnett, W. Clegg, R. E. Mulvey, P. A. O’Neil and D. Reed, *J. Organomet. Chem.*, 1996, **510**, 297–300.
- 26 M. Parvez, A. D. Pajerski and H. G. Richey Jr., *Acta Crystallogr., Sect. C: Cryst. Struct. Commun.*, 1988, **44**, 1212–1215.
- 27 N. D. R. Barnett, W. Clegg, A. R. Kennedy, R. E. Mulvey and S. Weatherstone, *Chem. Commun.*, 2005, 375–377.
- 28 P. C. Andrikopoulos, D. R. Armstrong, E. Hevia, A. R. Kennedy, R. E. Mulvey and C. T. O’Hara, *Chem. Commun.*, 2005, 1131–1133.
- 29 K. B. Starowieyski, J. Lewinski, R. Wozniak, J. Lipkowski and A. Chrost, *Organometallics*, 2003, **22**, 2458–2463.
- 30 W. Clegg, S. T. Liddle, R. E. Mulvey and A. Robertson, *Chem. Commun.*, 2000, 223–224.
- 31 G. M. Sheldrick, *Acta Crystallogr., Sect. A: Found. Crystallogr.*, 2008, **64**, 112–122.